Elsevier Editorial System(tm) for Experimental Thermal and Fluid Science
Manuscript Draft

Manuscript Number: ETFS-D-11-00485R1

Title: Micro-bubble generation rate and bubble dissolution rate into water by a simple multi-fluid mixer with orifice and porous tube

Article Type: Research Paper

Keywords: Micro-bubble, Mixer, Hydraulic performance, Bubble dissolution performance

Corresponding Author: Prof. Michio Sadatomi, Dr. of Engineering

Corresponding Author's Institution: Graduate School of Science and Technology, Kumamoto University

First Author: Michio Sadatomi, Doctor of Engineering

Order of Authors: Michio Sadatomi, Doctor of Engineering; Michio Sadatomi, Dr. of Engineering; AKIMARO KAWAHARA, Doctor of Engineering; Hidetoshi Matsuura, Master of Engineering; Shinji Shikatani, Master of Engineering

Abstract: A multi-fluids mixer by Sadatomi and Kawahara [1] is described as well as its performance as a micro-bubble generator for several trial products. In the experiments, air micro-bubble generation rate at water depths up to 3.6 m and the dissolution rates of oxygen in air and carbon dioxide into tap water at 20 ºC were measured. In the analyses, the micro-bubble generation rate data could be well predicted by Sadatomi et al.'s model [2] by choosing suitable energy loss coefficients needed in the model, and the oxygen dissolution rates in tap water could be well correlated with Kawahara et al.'s model [3]. The detail of the multi-fluid mixer and its practical significances together with a result of experiments and analyses are reported in the present paper.

December 14/2011

Dear Editor of Experimental Thermal and Fluid Science,

We want to submit our following paper to Experimental Thermal and Fluid Science.

Title: Micro-bubble generation rate and bubble dissolution rate into water by a simple multi-fluid mixer with orifice and porous tube

Authors: Michio Sadatomi [a], Akimaro Kawahara [a], Hidetoshi Matsuura [b] and Shinji Shikatani

[a] Graduate School of Science and Technology, Kumamoto University, Kumamoto, Japan

[b] Technology Research Division 5, Automobile R&D Center, Honda R&D Co., Ltd., Tochigi, Japan

[c] Mitsubishi Electric Corporation Kyoto Works, Manufacturing Control Department, Kyoto, Japan

Corresponding author:
Prof. Michio Sadatomi
Department of Advanced Mechanical System
Graduate School of Science and Technology, Kumamoto University
Kurokami 2-39-1, Kumamoto, 860-8555, Japan
sadatomi@mech.kumamoto-u.ac.jp
Phone & Fax +81-96-342-3757

Thank very much for editing of our paper.
Best regards,

Prof. Michio Sadatomi

*Highlights

Highlights

> The present author’s multi-fluids mixer is described together with its performance as a micro-bubble generator. > Micro-bubble generation rate at water depths up to 3.6 m and the dissolution rates of oxygen in air and carbon dioxide in tap water were measured. > The micro-bubble generation rate data could be well predicted by Sadatomi et al.’s model by choosing suitable energy loss coefficients needed in the model, and the dissolution rates in tap water could be well correlated with Kawahara et al.’s model.

Micro-bubble generation rate and bubble dissolution rate into water by a simple multi-fluid mixer with orifice and porous tube

Michio Sadatomi [a], Akimaro Kawahara [a], Hidetoshi Matsuura [b] and Shinji Shikatani

[a] Graduate School of Science and Technology, Kumamoto University, Kumamoto, Japan

[b] Technology Research Division 5, Automobile R&D Center, Honda R&D Co., Ltd., Tochigi, Japan

[c] Mitsubishi Electric Corporation Kyoto Works, Manufacturing Control Department, Kyoto, Japan

Keywords: Micro-bubble, Mixer, Hydraulic performance, Bubble dissolution performance.

ABSTRACT

A multi-fluids mixer by Sadatomi and Kawahara [1] is described as well as its performance as a micro-bubble generator for several trial products. In the experiments, air micro-bubble generation rate at water depths up to 3.6 m and the dissolution rates of oxygen in air and carbon dioxide into tap water at 20 ºC were measured. In the analyses, the micro-bubble generation rate data could be well predicted by Sadatomi et al.'s model [2] by choosing suitable energy loss coefficients needed in the model, and the oxygen dissolution rates in tap water could be well correlated with Kawahara et al.'s model [3]. The detail of the multi-fluid mixer and its practical significances together with a result of experiments and analyses are reported in the present paper.

Corresponding author:
Prof. Michio Sadatomi
Department of Advanced Mechanical System
Graduate School of Science and Technology, Kumamoto University
Kurokami 2-39-1, Kumamoto, 860-8555, Japan
sadatomi@mech.kumamoto-u.ac.jp
Phone & Fax +81-96-342-3757

1. Introduction

Micro-bubbles are tiny bubbles, less than a few hundred micrometers in diameter, and have several characteristics, such as high dissolubility in water around them. The most famous application of them is enriching oxygen into water in fisheries of oysters, pearl oysters and so on. Ohnari [4-6] reported that the enrichment promotes the oxygen consumption by the oysters etc. and their blood circulation and metabolism, resulting in the speed-up of their growth. Other applications of the micro-bubbles in industries and several micro-bubble generation methods are described in some books, say by Ueyama and Miyamoto [7].

Sadatomi [8, 9] invented a micro-bubble generator (MBG for short) with a spherical body in a flowing liquid tube and with a lot of drilled small holes on the tube for gas suction, in which micro-bubbles could be generated by supplying liquid alone because gas was automatically sucked by a negative pressure arisen behind the body. After that, Sadatomi et al. [2] proposed a model which can predict well the air micro-bubble generation rate by the MBG placed at any water depth, and Kawahara et al. [3] proposed a model which can predict well the dissolution rate of oxygen in air micro-bubbles into water and seawater. However, the MBG has two defects of (a) the difficulty of fixing the spherical body especially in smaller generator and (b) the troublesome drilling of a lot of small holes.

Recently, in order to overcome the above defects, Sadatomi and Kawahara [1] invented a new device with an orifice and a porous pipe instead of the spherical body and the small drilled holes. The new device is called a multi-fluids mixer in our laboratory because of multifunctional, which can generate (a) micro-bubbles by supplying liquid and sucking gas, (b) mists (i.e., tiny liquid droplets) by supplying gas and sucking liquid, and emulsion of immiscible liquids by supplying one of the liquids.

In the present paper, the structure of the multi-fluids mixer and its performance as a MBG are described for several trial products. In the experiments, three kinds of test were conducted: (a) hydraulic performance test of the present MBG, (b) bubble diameter measurement and (c) micro-bubbles dissolution performance test. In (a), air micro-bubble generation rate was measured at water depths up to 3.6 m by changing water supply rate to the MBG systematically. In (b) and (c), bubble diameter and the dissolution rate of oxygen into water through air micro-bubbles in 1.2 m deep water tank at 20 ºC and at atmospheric pressure were measured by changing both water supply rate and air suction rate systematically. In (c), the dissolution rate of carbon dioxide into water through carbon dioxide micro-bubbles was also measured. In the analyses, Sadatomi et al.'s model [2] is tested against the present micro-bubble generation rate data by choosing suitable energy loss coefficients needed in the model and Kawahara et al.'s model [3] is tested against the present dissolution rate data of oxygen in air bubbles. A result of such experiments and analyses together with the detail of the multi-fluid mixer and its practical significances are reported in the present paper.

Nomenclature

A_H total area of gas suction hole in porous pipe (m^2)
C concentration ($kg\ m^{-3}$)

D_L liquid-phase molecular diffusion coefficient ($m^2\ s^{-1}$)
d diameter of MBG pipe (m)
d_{BM} mean bubble diameter (m)
d_{BS} Sauter mean bubble diameter (m)
d_G diameter of gas suction hole in porous pipe (m)
d_o orifice diameter (m)
E_A ratio of oxygen dissolved into water to that supplied (dimensionless)
E_O Eotvos number (dimensionless)
f_C correction factor (dimensionless)
H water depth (m)
h_G thickness of porous pipe (m)
h_p height of bubble diameter measurement (m)
K_La volumetric mass transfer coefficient (s^{-1})
L_L water power (W)
l length of porous pipe (m)
N_C oxygen mass transfer rate ($kg\ s^{-1}$)
N number (dimensionless)
p gauge pressure (Pa)
Q volume flow rate ($m^3\ s^{-1}$)
T_L water temperature (°C)
t time (s)
u_B bubble rise velocity ($m\ s^{-1}$)
V volume (m^3)
v mean velocity ($m\ s^{-1}$)
W_{O2} mass flow rate of oxygen supplied to water ($kg\ s^{-1}$)

Greek symbols
β area ratio of orifice to MBG pipe (dimensionless)
ρ density ($kg\ m^{-3}$)
ζ energy loss coefficient (dimensionless)

Subscripts
E section far downstream from the exit
G gas
H homogeneous
L liquid
S saturation
1 inlet section of MBG
2 contraction section of MBG

2. Experiment

2.1. Micro-bubble generator

Fig. 1 shows the orifice type MBG [1] newly developed for the present experiment. The generator has an orifice in a flowing water tube. When pressurized water is introduced into the generator, the water velocity through the orifice becomes several times of that at the generator exit, thus from the energy conservation principle the pressure at a little downstream of the orifice becomes negative. With the aid of the negative pressure, air is automatically sucked through a porous pipe embedded in the pipe, and the air sucked is broken into a huge number of micro-bubbles by a high shear water flow with strong turbulence. Thus the generator can discharge a water jet with micro-bubbles from the exit.

Table 1 lists the specification of the orifice type MBG tested. The first three, named LP-8.8 to LP-14.6, are large types with the same stainless steel punched porous pipe except for the orifice diameter, d_o, being 8.8, 12.5 and 14.6 mm. The diameter of the circular tube was 22.0 mm; the area ratio of the orifice to the tube, β, was changed from 0.16 to 0.44 in order to study the effects of the area ratio; the length and the thickness of the porous pipe were l = 8 mm and h_G = 0.15 mm; the diameter of each punched holes was d_G = 300 μm, and the total area of the holes was A_H = 152.7 mm^2. The last three, SF-4.0 to LF-12.5, were geometrically similar to LP-12.5, but in order to study the effects of the MBG size the size of SF-4.0 and MF- 8.4 were around 1/3 and 2/3 of LF-12.5. In addition, SF-4.0 to LF-12.5 had the polyolefin (polypropylene polyethylene) fiber porous pipe with the porosity of d_G = 25 μm. The thickness and the length of the fiber porous were h_G = 1.5 mm and l = 3 to 8 mm depending upon the pipe size.

2.2. Test apparatus and measurement systems

Three kinds of test were conducted: (a) hydraulic performance test, (b) bubble diameter measurement test and (c) micro-bubbles dissolution performance test. Fig. 2 shows the present test apparatus and measurement systems. Two water tanks were used as the test water tank: a small transparent acrylic resin water tank with 2.0 m in height and 0.30 m in diameter, and a large opaque poly-vinyl-chloride water tank with 4.0 m in height and 0.489 m in diameter. Water was circulated with a centrifugal pump from the bottom of the tank to the MBG in the tank via a flow control valve and a calibrated magnetic flow meter for the measurement of water volume flow rate, Q_L. The air suction rate into the MBG, Q_G, was measured with a calibrated mass flow meter. The uncertainties in the measurements of Q_L and Q_G are about 1 % and about 3 %, respectively.

2.3. Hydraulic performance test

In order to familiarize the present MBG to various application fields, the generation rate of the micro-bubbles has to be predictable, depending upon the water depth of MBG placed and water supply rate to the MBG. In addition, a pumping power to supply water to the MBG must be predictable. So, the hydraulic performance test was conducted to obtain experimental data necessary to validate the performance prediction model [2]. In the test, in order to study the effects of water depth of the MBG in the water tank, H, H was changed as 0.4, 0.8, 1.2 m in the small water tank and 2.4 and 3.6 m in the large water tank, and the needle valve in the air suction line was full opened. The water supply rate to the MBG, Q_L, was varied up to 106 l/min depending upon both the MBG size and the MBG depth from the water surface, while the air suction rate, Q_G, was changed up to 21 l/min depending upon Q_L. In addition to the measurements of Q_L and Q_G mentioned in 2.2, the air pressure, p_G, and the water pressure, p_L, at the MBG inlet were also measured with two different pressure transducers calibrated within the uncertainties of 50 Pa. As shown in Fig. 2, the output signals from the above mentioned flow rate and pressure sensors were fed to a personal computer via an A/D converter to determine the respective time-averaged values. The water power needed to generate micro-bubbles by the MBG, L_L, was calculated by substituting the measured p_L and Q_L, and the mean water velocity at the MBG inlet, v_{L1}, into Eq. (1).

$$L_L = (p_L + \rho_L v_{L1}^2/2)Q_L \tag{1}$$

2.4. Bubble diameter measurement

The bubble diameter is known to affect the rising velocity and the dissolution performance of the bubble. So, filling water to H = 1.2 m in the small transparent tanked, we measured bubble diameter with a high-speed video camera and an image processing system. Bubble images against a back flash light at h_p = 0.6 m were taken with the video camera at a shutter speed of 1/30,000 s. 100- and 30-power microscope lenses, corresponding to 2.32 mm and 7.73 mm in frame height, were attached to the camera for measuring smaller and larger bubbles than 0.1 mm. The minimum measurable bubble diameter was 0.01 mm, thus the uncertainty of the bubble diameter measurement is 0.01 mm. The number of pictures taken was so determined that the total frame area captured becomes identical between the smaller and the larger frames. In the bubble diameter measurement, although most of the bubbles were spherical the major and the minor axes of the bubble on pictures were measured for distorted bubbles larger than 1.5 mm, and averaged value of the two axes was taken as the bubble diameter. In order to obtain reliable bubble diameter distribution, more than 350 bubble diameters were measured, and the mean and the Sauter mean bubble diameters were calculated by

$$d_{BM} = \frac{\sum n_i d_{Bi}}{\sum n_i},\ d_{BS} = 6 \times \frac{\sum\left(n_i \pi d_{Bi}^3/6\right)}{\sum n_i \pi d_{Bi}^2} \tag{2}$$

Here, n_i is the number of bubbles classified in a bubble diameter range of d_{Bi}.

2.5. Micro-bubble dissolution performance test

Enrichment of oxygen into water through air micro-bubbles is very important in fisheries, sewage treatment system etc. So, the micro-bubble dissolution test was conducted with the small water tank by filling 0.13 m^3 tap water, corresponding to H = 1.2 m. The test liquid was tap water, while the test gas was air from atmosphere or the carbon dioxide from a CO_2 cylinder. The water supply rate to the MBG, Q_L, was limited to 72 l/min, and air or carbon dioxide suction rate to 4 l/min. The water temperature, T_L, was kept at 20 ± 0.1 °C using a cooling system in the experiment, because it affects bubble dissolution characteristics. Salinity effects were not studied in the present study because the study will be done as a future work.

Most tests were conducted with air as the test gas. Firstly, nitrogen gas was blown into water in order to reduce the oxygen dissolved in water, DO, to about 4 mg/l because water from our laboratory source always showed a high DO value at the beginning and the time to reduce it to zero is too long. Secondary, air was blown as micro-bubbles through MBG at assigned flow rates of air and water, and the time variation of oxygen concentration in water, C, was measured with a DO meter (OE-270AA and MM-60, DKK-TOA Co.) within the uncertainties of 0.02 mg/l. The volumetric mass transfer coefficient, K_La, was determined from the time variation data by fitting Akita and Yoshida's equation [10]:

$$dC/dt = K_La(C_S - C) \tag{3}$$

Here, C and C_S are the concentration of dissolved oxygen at a time t and at saturation, respectively. In addition, in order to confirm a well-mixed condition, we measured C at the bottom, the middle and the top of the test tank, and confirmed C values at the three positions to be similar within the accuracy of DO measurement. As a result, K_La could be determined within the uncertainty of about 10 %.

Oxygen absorption efficiency, E_A, the ratio of the oxygen dissolved in water to that supplied to, is calculated from:

$$E_A = \frac{N_C}{W_{O_2}} \times 100\ \% \tag{4}$$

Here, W_{O2} is the mass flow rate of oxygen supplied to water as air bubbles, being 23% of air mass flow rate supplied. N_C is the oxygen mass transfer rate given by

$$N_C = K_LaV_LC_S \tag{5}$$

Here, V_L is the volume of water in the test tank.

Similar measurements were also conducted for carbon dioxide, CO_2, micro-bubbles instead of air micro-bubbles. The time variation in CO_2 concentration in water was measured with a CO_2 meter (Ti-9004, Toko Kagaku Co.) within the uncertainty of 2.2 mg/l. K_La was determined by substituting the time variation data on the concentration of carbon dioxide into Eq. (3). As a result, K_La could be determined within the uncertainty of about 10 %. Furthermore, E_A was determined from Eqs. (4) and (5), though W_{O2} and C_S must be replaced by the values for carbon dioxide. In addition, K_La so determine for carbon dioxide micro-bubbles was compared with that for air micro-bubbles.

3. Results and discussion

3.1. Hydraulic performance

Figs. 3 (a) to (c) show typical results of hydraulic performance tests for the large size, punched porous type MBG of LP-8.8, LP-12.5 and LP-14.6, each different in orifice diameter but the other sizes were the same. The MBG depth in the water tank in Fig. 2 was set at H = 0.4 to 3.6 m, and the needle valve in the air suction line was full opened. Unfortunately, however, LP-8.8 did not work at H = 2.4 and 3.6 m because the water pressure required at the MGB inlet was higher than that given by the present water circulation pump.

Fig. 3 (a) shows the data of air suction rate, Q_G, against the water supply rate, Q_L. The data points are labeled with different symbols according to both the MGB type and the water depth, H. In addition, data point in each MBG type at H = 0.4 m is connected each other with line segments, to facilitate the understanding of the trend of data. With increasing of Q_L at a fixed H, the water gauge pressure in the air suction section downstream of the orifice decreases from positive to negative. After that, Q_G

increases steeply with increasing of Q_L. In addition, Q_G increases with decreasing of H because the water pressure at the MBG exit decreases and thus the water pressure in the air suction section decreases. Among these three types, LP-8.8 gives the largest Q_G at a fixed Q_L because the water pressure in the air suction section becomes the lowest at a fixed Q_L.

Fig. 3 (b) shows the data of gauge pressure at the MGB water inlet, p_L, against the water supply rate, Q_L. p_L in each MBG is almost proportional to Q_L^2, and p_L increases with decreasing of the orifice diameter, because the pressure drop through the MBG increases with decreasing of the orifice diameter at a fixed Q_L.

Fig. 3 (c) shows Q_G data against the water power, L_L, calculated from Eq. (1). The line tangent to the data through the origin is steeper the more efficient because the ratio of micro-bubble generation rate to the power required becomes high. Therefore, LP-14.6 and LP-12.5 is superior to LP-8.8 at $H < 1.2$ m, and the maximum attainable Q_G was higher in LP-12.5 than LP-14.6. In addition, the mean and the Sauter mean bubble diameters, d_{BM} and d_{BS}, measured for LP-12.5 under several Q_L and Q_G conditions were 1/3 to 1/2 of those for LP-14.6. Thus, LP-12.5 is superior to LP-14.6 at $H < 1.2$ m. At $H > 2.4$ m, on the other side, LP-14.6 is superior to LP-12.5. However, our previous study [11] demonstrated that for the use of MBG in deep water the supply of pressurized air to the MBG is more efficient than the suction of air by the increment of water supply rate. This means that the superiority in deep water of $H > 2.4$ m is not important. Thus, LP-12.5, being the diameter ratio of orifice to MGB pipe to be 0.57, is recommended as a whole.

Figs. 4 (a) and (b) show typical results of hydraulic performance tests for the fiber porous type MBG of LF-12.5, MF-8.4 and SF-4.0, each different in size but the proportion of orifice diameter to pipe diameter, etc. was the same as that for LP-12.5. Thus, the size effects of the MBG can be studied by comparing these three.

Fig. 4 (a) shows Q_G data against Q_L. The trend of Q_G against Q_L and H is similar to Fig. 3 (a). It is mysterious that the maximum Q_G for LF-12.5 and MF-8.4 is nearly the same and limited to 15 l/min at $H = 0.4$ m. The reason is probably due to a partial water immersion in fiber porous especially for LF-12.5.

Fig. 4 (b) compares Q_G data against the water power, L_L at $H = 1.2$ m. In order to know the effects of the number of the MBG placed in the same water depth, the data for double uses of SF-4.0 and MF-8.4 are also plotted and connected with broken line segments. It is seen that the double use of SF-4.0 is efficient if the demand of Q_G is less than 9 l/min at $H = 1.2$ m, and the double use of MF-8.4 is efficient if the demand of Q_G is between 9 l/min and ca. 17 l/min.

Fig. 5 compares Q_G data between LP-12.5 and LF-12.5 (thickened symbols), being different in porous material. Though the diameter of air suction hole for LP-12.5 is 300 μm and that for LF-12.5 is 25 μm, the difference of Q_G between them is small, because the number of the hole is much more for LF-12.5 than LP-12.5.

3.2. Bubble diameter

Figs.6 (a) and (b) show typical bubble diameter distribution data for LP-12.5 and LF-12.5, being different in porous material, at Q_L = 67 and 66 l/min and at H = 1.2 m. In each figure, the data at Q_G = 1.0 l/min and 4.0 l/min are compared each other, and the mean and the Sauter mean bubble diameter data, and the total number of bubbles measured were also shown. In the bubble diameter measurement test and bubble dissolution test, in order to control the air suction rate, Q_G, at a prescribed value, the needle valve in air line in Fig. 2 was partially closed. The diameter of each bubble was classified from 0.01 – 0.05 to 3.0 – 4.0 mm. Though the bubbles smaller than 0.01 mm could not be measured in the present experiment, such an extremely smaller bubble may exist. Excluding smaller bubbles than 0.01 mm, more than 70 % bubbles are smaller than 0.1 mm. At Q_G = 1.0 l/min, the mean bubble diameter and the Sauter mean bubble diameter are respectively around 0.12 mm and 0.63 mm, and larger bubbles than 2.0 mm did not exist, independent of porous materials. At Q_G = 4.0 l/min, however, 3.0 – 4.0 mm bubbles existed, and caused the enlargement of the Sauter mean bubble diameter. Similar trend of data was obtained for other MBG types. Thus, in order to generate micro-bubbles alone, Q_G must be lower than 1.0 l/min in the present MBG types. However, even at Q_G = 4.0 l/min, the present MBG are usable as a micro-bubble generator because most bubbles are smaller than 0.1 mm.

Fig. 6 (c) shows the effects of water supply rate, Q_L, on the Sauter mean bubble diameter data at Q_G = 1.0 l/min and 4.0 l/min. As anticipated from Fig.3 (a) and Fig. 4 (a), Q_L for each MBG type could not be changed in a wide range at H = 1.2 m. So, the mean water velocity at orifice, v_{L2} (= 4 Q_L / (π d_O^2)), is taken as the abscissa. With increasing of v_{L2}, the Sauter mean bubble diameter, d_{BS}, decreases, and over about v_{L2} = 9 m/s it becomes a similar value independent of v_{L2} and MBG type but dependent on Q_G. Thus, in order to generate micro-bubbles alone by the present MBG, v_{L2} should be higher than 10 m/s.

3.3. Bubble dissolution performance

Figs. 7 (a) and (b) show typical variation of oxygen and carbon dioxide concentrations in tap water after bubbling of air and carbon dioxide, respectively.

In the air bubbling case, in order to reduce the initial oxygen concentration to about 4 mg/l, the pre-bubbling of nitrogen gas was conducted at first. Then, air bubbling was conducted, and the concentration goes up gradually to the saturation value of C_S = 8.84 mg/l at 20 °C, and the arrival time to the saturation is about 10 minute at Q_G = 4.0 l/min and about 35 minute at Q_G = 1.0 l/min. By fitting these data to Eq. (3), we obtained the volumetric mass transfer coefficient, K_La. In addition, we obtained the oxygen absorption efficiency, E_A, by substituting K_La data etc. into Eqs. (4) and (5).

In carbon dioxide bubbling case, pre-bubbling of any gas was not needed since the initial CO_2 concentration is near to zero. Since the saturation concentration of carbon dioxide is C_S = 1724 mg/l, being much higher than that of oxygen, the increase of the concentration is very slow, and the arrival time to the saturation value could not be detected. In addition, K_La for carbon dioxide case is very low and about one-seventh to one-eleventh of that for oxygen case.

Figs. 8 (a) and (b) show K_La data against Q_G and L_L, respectively. Data are labeled according to the MGB type, water supply rate to the MGB and dissolved gas (open symbol for oxygen, darkened symbol for carbon dioxide). As is noticed from Fig. 8 (a), K_La for the oxygen case (open symbols) increases linearly with Q_G irrespective of the orifice diameter, the porous pipe, the MBG size and the water flow rate, Q_L. A similar trend is seen for the carbon dioxide case (darkened symbols). In Fig. 8 (b), the maximum value of K_La data at a fixed Q_L in each MBG is plotted against the water power, L_L, with the same symbol as seen in Fig. 8 (a). Since the ratio of K_La to L_L is considered to be one of the indices of efficiency, the line tangent to the data through the origin is steeper the more efficient. Thus, LP-12.5 and LP-14.6 types with punched porous at a higher liquid supply rate of Q_L = 67 and 72 l/min are superior to others included LF-type with fiber porous. The main reason of this is that the maximum Q_G is larger in these LP-types. In addition, the present data are compared with those obtained by Terasaka et al. [12] for four kinds of MBG: spiral liquid flow type (Nanoplanet Co., Ltd.) [5], ejector type (Aura Tech Co., Ltd.), Venturi type (Watanabe et al. [13]) and pressurized dissolution type (Shigenkaihatsu Co., Ltd.). Of these four types, spiral liquid flow type showed best performance in L_L < 240 W [12], so the range of data for spiral liquid flow type is drawn on Fig. 8 (b). From the comparison in Fig. 8 (b), LP-12.5 and LP-14.6 types in the present MBG are superior to spiral liquid flow type and the other types tested by Terasaka et al. [12].

Fig. 9 compares E_A data mainly for the oxygen case. The effects of MBG type on E_A are relatively small. E_A for all cases are almost 25 to 30 %, but decrease a little as Q_G increases. The difference in E_A between the oxygen case and the carbon dioxide case is small because in Eq. (5) K_La is smaller but C_S is larger for carbon dioxide case than for oxygen case.

4. Test of prediction model

4.1. Hydraulic performance

Sadatomi et al. [2] proposed a model which can predict well the micro-bubble generation rate for the spherical body-type MBG (Sadatomi et al. [8, 9]) placed at any water depth. In the model, the following energy equations are simultaneously solved.

Liquid inlet ↔ Confined point:

$$p_L + \frac{\rho_L v_{L1}^2}{2} = p_2 + \frac{\rho_L v_{L2}^2}{2} + \zeta_1 \frac{\rho_L v_{L1}^2}{2} \tag{6}$$

Confined point ↔ Point far from exit:

$$p_2 + \frac{\rho_L v_{L2}^2}{2} = p_3 + \zeta_2 \frac{\rho_H v_H^2}{2} \tag{7}$$

Gas inlet ↔ Confined point:

$$p_2 + \frac{\rho_G v_{G2}^2}{2} = p_G - \zeta_3 \frac{\rho_G v_{G2}^2}{2} \tag{8}$$

Here, p_L, p_2, p_3 and p_G are the static pressures, respectively at the liquid inlet, the confined point, the point far from the exit and the gas inlet. v_{L1}, v_{L2} and v_{G2} are the mean velocities at the liquid inlet, the confined point and the gas inlet. ρ_L and ρ_G are the densities of the liquid and the gas. ζ_1, ζ_2 and ζ_3 are the energy loss coefficients which must be determined from experimental data as described more detail in Ref. [2], and their values for the present MBG are listed in Table 2. ρ_H and v_H are the density and the velocity of the homogeneous mixture of the micro-bubbles and water, defined as:

$$\rho_H = \frac{\rho_G Q_G + \rho_L Q_L}{Q_G + Q_L}, \qquad v_H = \frac{Q_G + Q_L}{\pi D^2/4}. \tag{9}$$

The calculated results by the above model are compared with the present data on the present MBG with the orifice and the porous pipe. Figs. 10 (a) and (b) are the examples of such a comparison for the micro-bubble generation rate, Q_G, and the gauge pressure at the MBG liquid inlet, p_L. The agreement between the calculated curves and the experimental data points is good. Thus, if we want to generate micro-bubble at an arbitrary flow rate and at any water depth, we can evaluate the water supply rate to the MBG and the gauge pressure at the MBG inlet by the model, thus we can select the optimum pump for supplying water to the MBG.

4.2. Bubble dissolution into water

Kawahara et al. [3] proposed a correlation of correction factor, f_C, in the following Nedeltchev et al.'s K_La correlation [14]:

$$K_L a = f_C \sqrt{\frac{4D_L u_B}{\pi d_{BS}} \frac{6Q_G H}{V d_{BS} u_B}} \tag{10}$$

Here, D_L is the liquid-phase diffusion coefficient, and u_B the bubble velocity, d_{BS} the Sauter mean bubble diameter, H the depth of the liquid phase in the bubble column, and V the total volume of the gas and the liquid in the bubble column.

Nedeltchev et al. [14] proposed an f_C correlation for milli-bubbles of $1.7 < E_O < 7$ as:

$$f_C = 0.185 E_O^{0.737} \tag{11}$$

Here, Eo is the Eotvos number defined by,

$$E_O = \frac{g d_{BS}^2 (\rho_L - \rho_G)}{\sigma} \tag{12}$$

Kawahara et al. [3] obtained an f_C correlation for micro-bubbles of $0.006 < E_O < 0.55$ in $Q_G \leq 4$ l/min in tap water and salt water generated by the spherical body-type MBG as:

$$f_C = 2.36 E_O^{0.735}. \tag{13}$$

Since micro-bubble diameter in tap water was 5 to 10 times larger than that 3 wt % salt water [3], the range of E_O for the present micro-bubbles in tap water was $0.08 < E_O < 0.77$ and biased to higher E_O side than that in [3]. Since f_C by Eq. (13) is 40 % higher at maximum for the present micro-bubbles, so for the present micro-bubbles we modified f_C further by

$$f_C = 1.69 E_O^{0.72}. \tag{14}$$

Fig. 11 compares K_La between the calculations by Eqs. (10), (12) and (14) and the present experimental data in $Q_G \leq 4$ l/min for the 14 combinations of the MBG types and Q_L, where the MBG was placed at H = 1.2 m in water depth. In the calculation, the present experimental data of d_{BS} and u_B were given as the input data. Irrespective of the orifice size, the MBG size and the porous type, the data are well predicted by the calculations within ± 20 %.

5. Concluding remarks

The generation and the dissolution of micro-bubbles in tap water were studied for a newly developed MBG with orifice and porous pipe. From the experiments of the six kinds of trial products with different orifice diameter, different porous pipe and different MBG size together with the analyses of the data, the followings have been clarified:

(1) As the diameter ratio of orifice to pipe in the present MGB, about 0.57, corresponding to LP-12.5, SF-4.0, MF-8.4 and LF-12.5 types, is recommended since the ratio of micro-bubble generation rate to power consumption rate was higher at H < 1.2 m and the maximum attainable bubble generation rate was higher.

(2) Mean bubble diameter and Sauter mean bubble diameter for the present MBG was around 0.12 mm and 0.63 mm at Q_G = 1.0 l/min if the mean water velocity through the orifice is higher than about 10 m/s. No appreciable effects on bubble diameter are seen between the 300 μm punching porous and 25 μm fiber porous.

(3) The volumetric mass transfer coefficient, K_La, increased linearly with Q_G, independent of Q_L and MBG type, and is higher for the punching porous type than the fiber porous type. K_La for the carbon dioxide was very low, about one-seventh to one-eleventh of that for oxygen.

(4) For the ratio of K_La to L_L, one of the indicies of efficiency, the present LP-12.5 and LP-14.6 types are superior to four kinds of MBG tested by Terasaka et al. [12] including spiral liquid flow type MBG.

(5) The ratio of oxygen dissolved in water to that supplied, E_A, was almost 25 to 30 %, roughly independent of Q_G and MBG type in Q_G < 10 l/min.

(6) The micro-bubble generation rate could be well predicted by the Sadatomi et al.'s model [2] by giving the experimentally determined energy loss coefficients, ζ_1, ζ_2 and ζ_3 as input data.

(7) The air micro-bubble dissolution rate in tap water could be well predicted by the Kawahara et al.'s model [3] by lowering the correction factor by about 40 %.

All conclusions mentioned above are effective within the present experimental range. So, in order to validate the present conclusions to other cases, further studies are needed. In addition, it is very important to construct a model applicable to the dissolution of carbon dioxide in water and sea water from a global warming protection point of view.

Acknowledgements

The authors would like to express their heartfelt gratitude to Mr. K. Ariyoshi, a technician at Kumamoto Univ., for manufacturing the MBG, etc., and Mr. M. Noguchi and Mr. M. Kato, students in those days for their experimental cooperation. Financial supports from JSPS KAKENHI (21560181), Harada Memorial Foundation and Big-Bio Co. are also appreciated.

References

[1] M. Sadatomi, A. Kawahara, Fluids mixer and fluids mixing method, Japanese Patent, JP. 2008-173631, 2008.

[2] M., Sadatomi, A. Kawahara, F. Matsuyama, T. Kimura, An advanced micro-bubble generator and its application to a newly developed bubble-jet type air-lift pump, Multiphase Science and Technology 19 (2007) 323–342.

[3] A. Kawahara, M. Sadatomi, F. Matsuyama, H. Matsuura, M. Tominaga, M. Noguchi, Prediction of micro-bubble dissolution characteristics in water and seawater, Experimental Thermal and Fluid Science 33 (2009) 883–894.

[4] H. Ohnari, Waste water purification in wide water area by use of micro-bubble techniques (in Japanese), Japanese Journal of Multiphase Flow 11 (1997) 263–266.

[5] H. Ohnari, T. Saga, K. Watanabe, K. Maeda, High functional characteristics of micro-bubbles and water purification (in Japanese), Resources Processing 46 (1999) 238–244.

[6] H. Ohnari, Fisheries experiments of cultivated shells using micro-bubbles technique (in Japanese), Journal of the Heat Transfer Society of Japan 40 (2001) 2–7.

[7] T. Ueyama, M. Miyamoto, World of micro-bubbles – Cooperative action of water and gas (in Japanese), Kougyoutyousakai, Tokyo, 2006.

[8] M. Sadatomi, A. Kawahara, K. Kano, A. Ohtomo, Performance of a new micro-bubble generator with a spherical body in a flowing water tube, Experimental Thermal and Fluid Science 29 (2005) 615–623.

[9] M. Sadatomi, Micro-bubble generator, Japanese Patent 4069211, 2008.

[10] K. Akita, F. Yoshida, Gas holdup and volumetric mass transfer coefficient in bubble columns, Industrial and Engineering Chemistry, Process Design and Development 12 (1973) 76–80.

[11] M. Sadatomi, A. Kawahara, T. Goto, Experiment and performance prediction of a bubble-jet-type air-lift-pump for dredging sediments, Proceedings of 7th Int. Conf. on Heat Transfer, Fluid Mechanics and Thermodynamics (July 2010), held in Antalya, Turkey, 6 pages in CD-ROM.

[12] K. Terasaka, A. Hirabayasshi, T. Nishino, S. Fujioka, D. Kobayashi, Development of microbubble aerator for waste water treatment using aerobic activated sludge, Chemical Engineering Science 66 (2011) 3172–3179.

[13] Watanabe, K., Fujiwara, A., Takagi, S., Matsumoto Y., The experimental study of micro-bubble generator by Venturi tube (in Japanese), Proceedings of the Annual Meeting of the Japanese Society for Multiphase Flow (August 2004) 185–186.

[14] S.Nedeltchev, U. Jordan, A. Schumpe, A new correction factor for theoretical prediction of mass transfer coefficients in bubble columns, Journal of Chemical Engineering of Japan 39 (2006) 1237–1242.

List of Figures

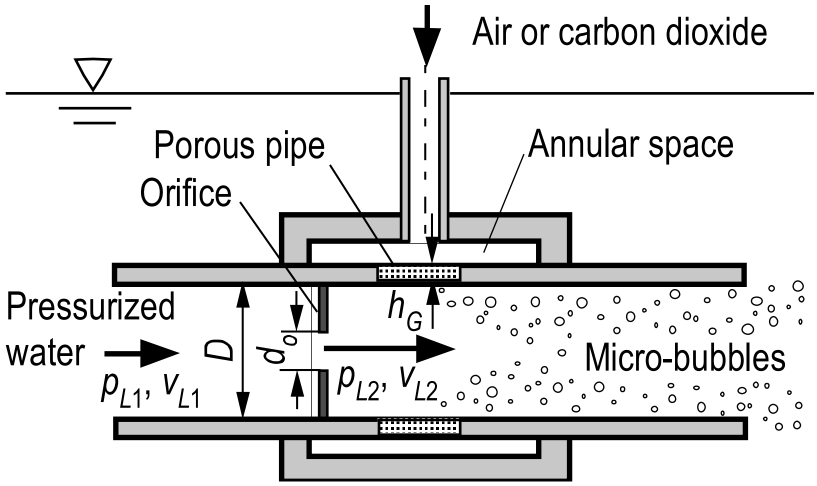
Air or carbon dioxide
Porous pipe
Annular space
Orifice
Pressurized
water
p_{L1}, v_{L1}
D
d_o
h_G
p_{L2}, v_{L2}
Micro-bubbles

Fig. 1.

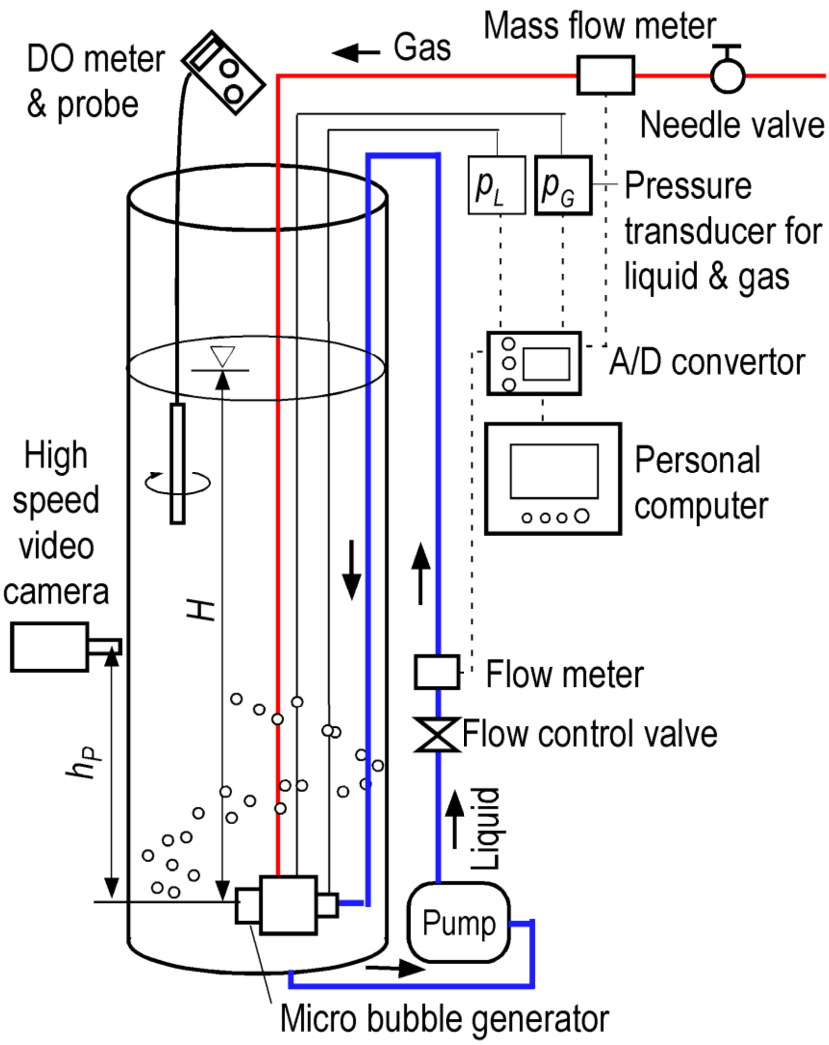

DO meter
& probe
Gas
Mass flow meter
Needle valve
p_L
p_G
Pressure
transducer for
liquid & gas
A/D convertor
Personal
computer
High
speed
video
camera
H
h_P
Flow meter
Flow control valve
Liquid
Pump
Micro bubble generator

Fig. 2.

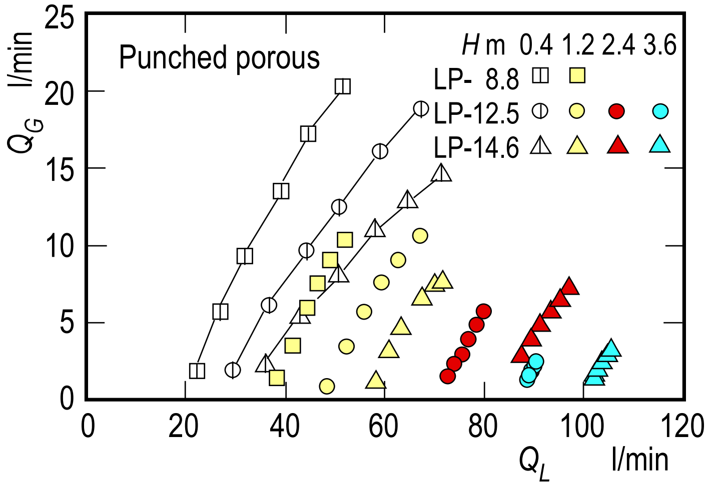
Punched porous
H m 0.4 1.2 2.4 3.6
LP- 8.8
LP-12.5
LP-14.6
Q_G l/min
0 5 10 15 20 25
0 20 40 60 80 100 120
Q_L l/min

(a)

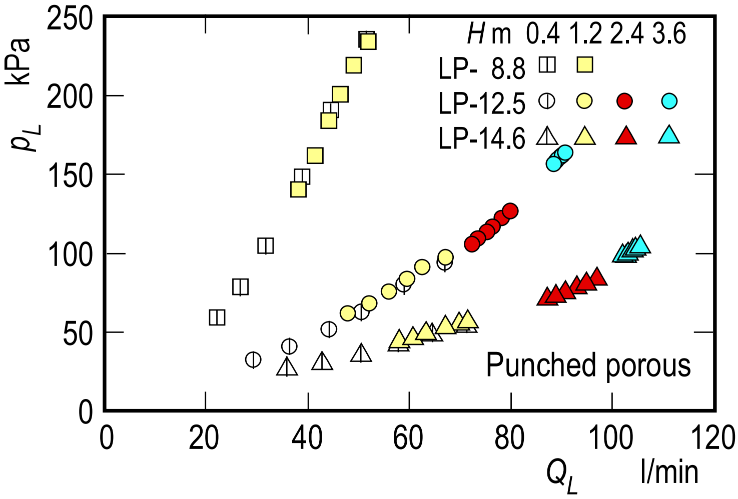
H m 0.4 1.2 2.4 3.6
LP- 8.8
LP-12.5
LP-14.6
Punched porous
p_L kPa
0 50 100 150 200 250
0 20 40 60 80 100 120
Q_L l/min

(b)

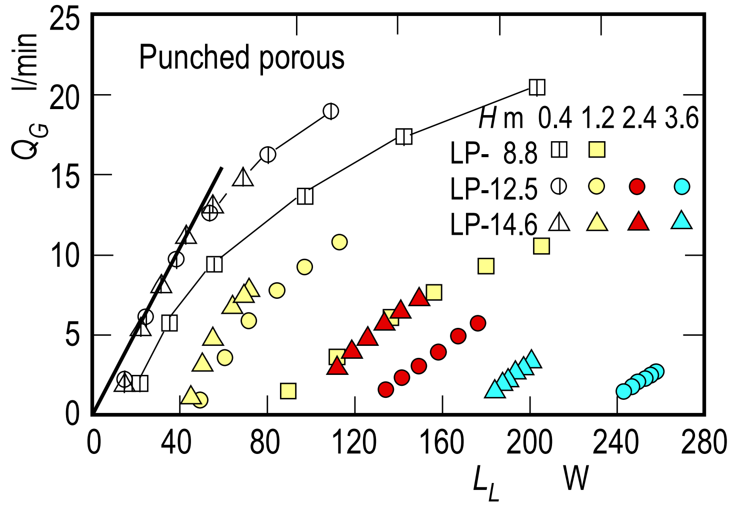
Punched porous
H m 0.4 1.2 2.4 3.6
LP- 8.8
LP-12.5
LP-14.6
Q_G l/min
0 5 10 15 20 25
0 40 80 120 160 200 240 280
L_L W

(c)

Fig. 3.

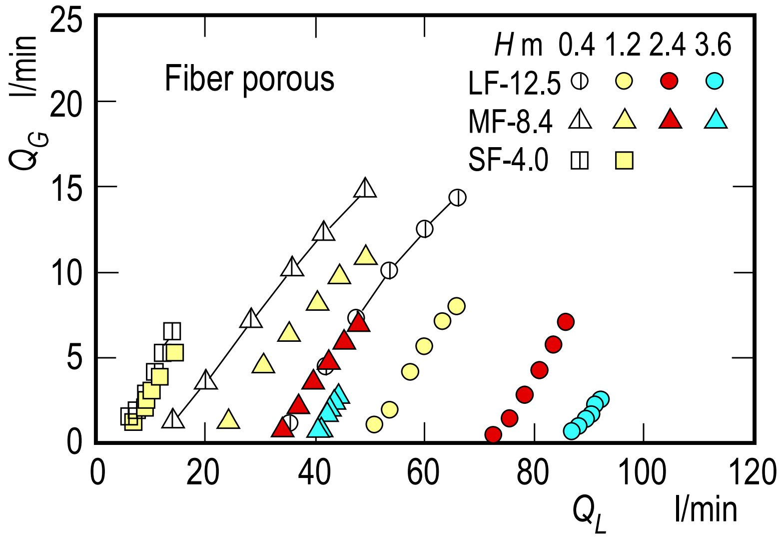

Fiber porous
H m 0.4 1.2 2.4 3.6
LF-12.5
MF-8.4
SF-4.0
Q_G l/min
Q_L l/min
0
5
10
15
20
25
0
20
40
60
80
100
120

(a)

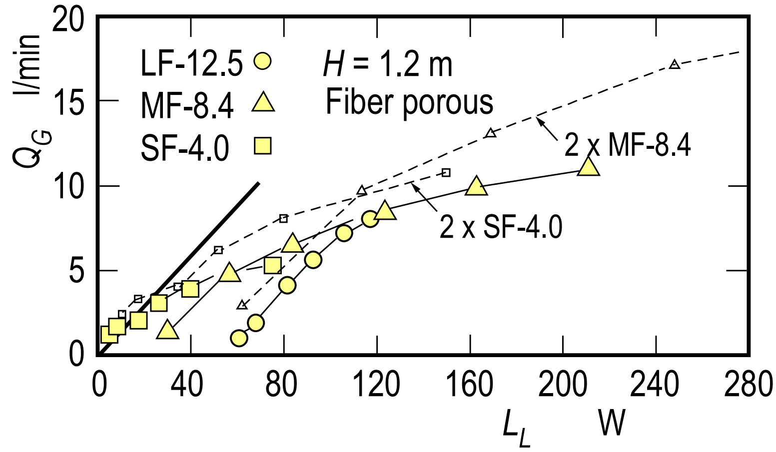

LF-12.5
MF-8.4
SF-4.0
H = 1.2 m
Fiber porous
2 x MF-8.4
2 x SF-4.0
Q_G l/min
L_L W
0
5
10
15
20
0
40
80
120
160
200
240
280

(b)

Fig. 4.

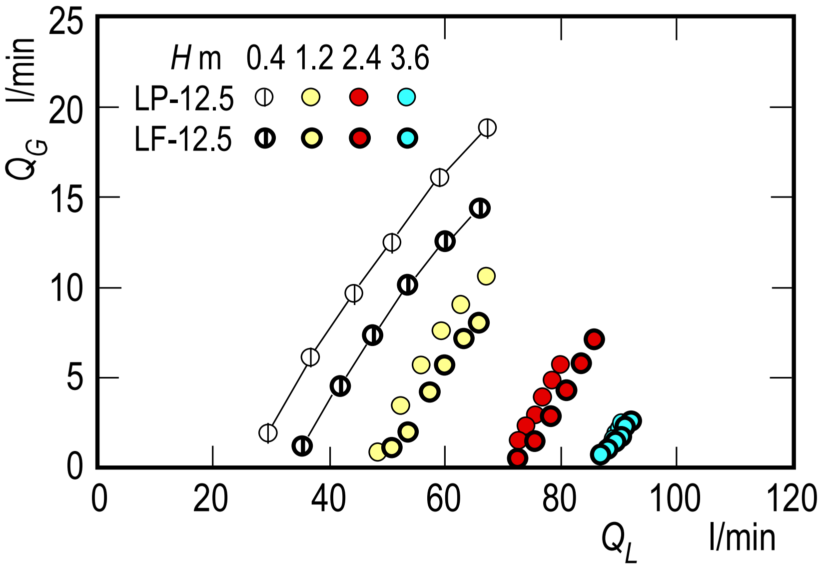

Q_G l/min
25
20
15
10
5
0
H m 0.4 1.2 2.4 3.6
LP-12.5
LF-12.5
0
20
40
60
80
100
120
Q_L l/min

Fig. 5.

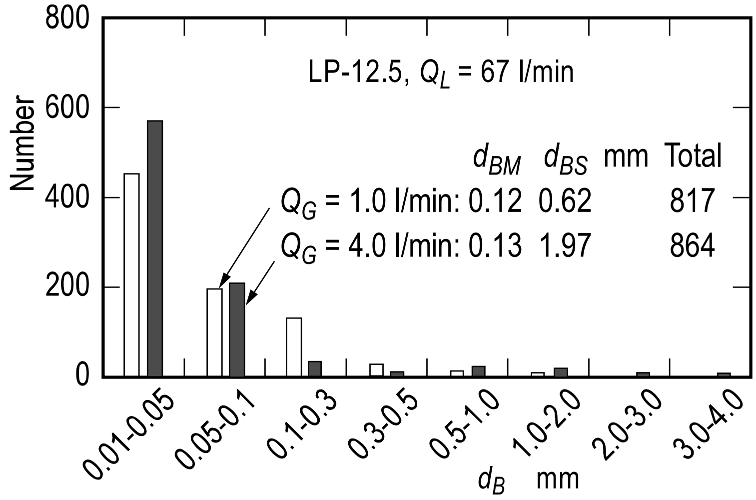
LP-12.5, Q_L = 67 l/min
d_{BM} d_{BS} mm Total
Q_G = 1.0 l/min: 0.12 0.62 817
Q_G = 4.0 l/min: 0.13 1.97 864
Number
d_B mm
0.01-0.05
0.05-0.1
0.1-0.3
0.3-0.5
0.5-1.0
1.0-2.0
2.0-3.0
3.0-4.0

(a)

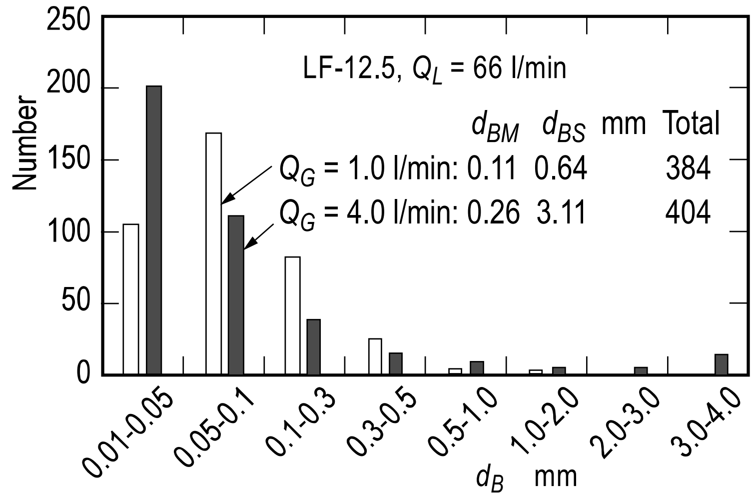
LF-12.5, Q_L = 66 l/min
d_{BM} d_{BS} mm Total
Q_G = 1.0 l/min: 0.11 0.64 384
Q_G = 4.0 l/min: 0.26 3.11 404
Number
d_B mm
0.01-0.05
0.05-0.1
0.1-0.3
0.3-0.5
0.5-1.0
1.0-2.0
2.0-3.0
3.0-4.0

(b)

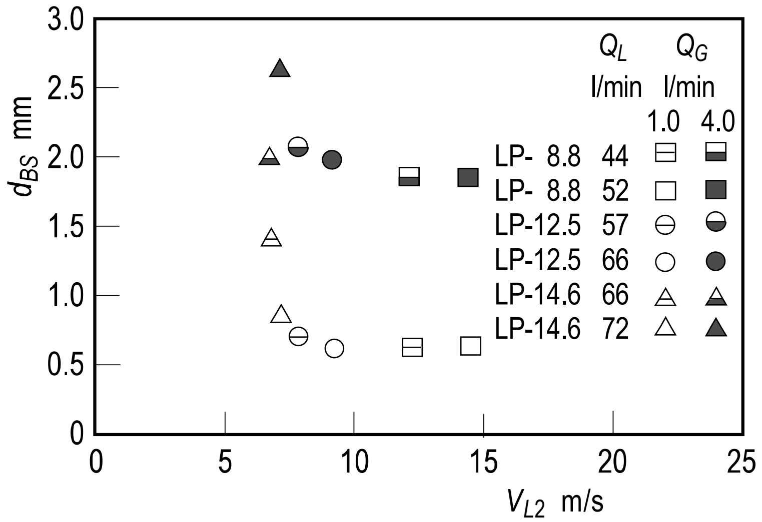
Q_L l/min
Q_G l/min
1.0 4.0
LP- 8.8 44
LP- 8.8 52
LP-12.5 57
LP-12.5 66
LP-14.6 66
LP-14.6 72
d_{BS} mm
V_{L2} m/s

(c)

Fig. 6.

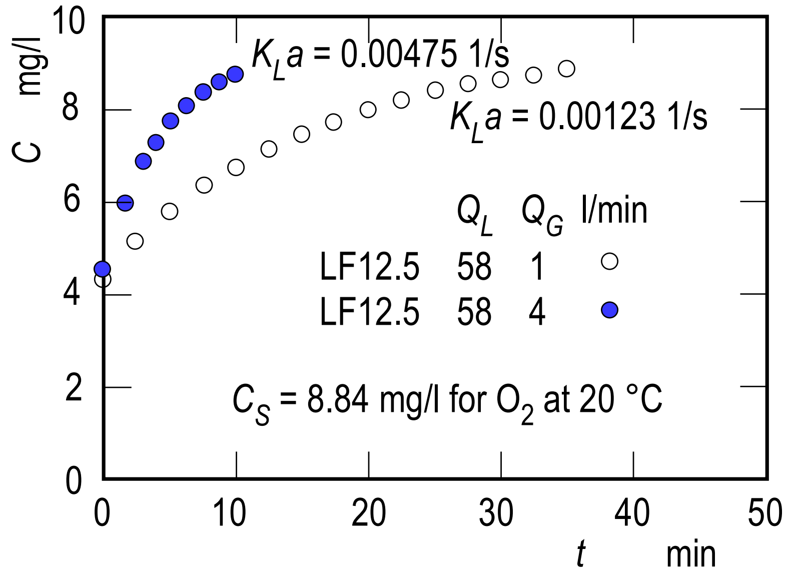

C mg/l
t min
K_La = 0.00475 1/s
K_La = 0.00123 1/s
Q_L Q_G l/min
LF12.5 58 1
LF12.5 58 4
C_S = 8.84 mg/l for O_2 at 20 °C

(a)

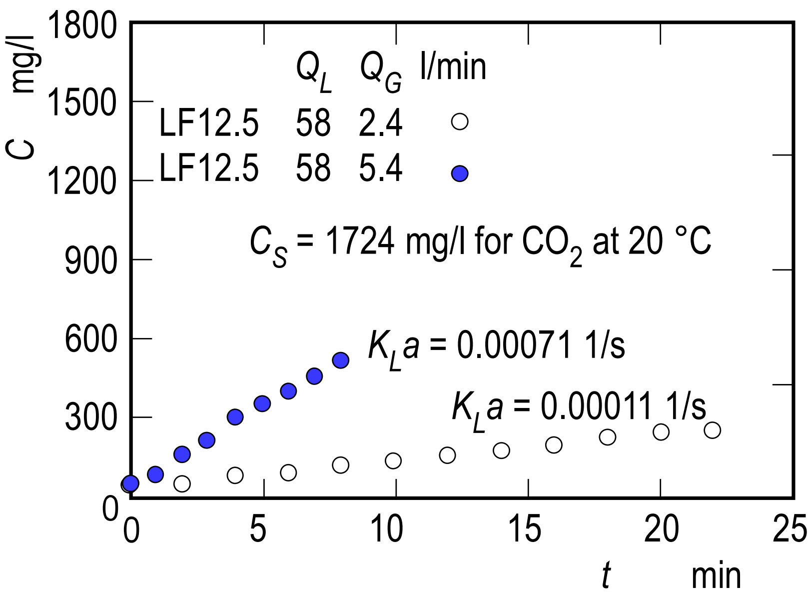

C mg/l
t min
Q_L Q_G l/min
LF12.5 58 2.4
LF12.5 58 5.4
C_S = 1724 mg/l for CO_2 at 20 °C
K_La = 0.00071 1/s
K_La = 0.00011 1/s

(b)

Fig. 7.

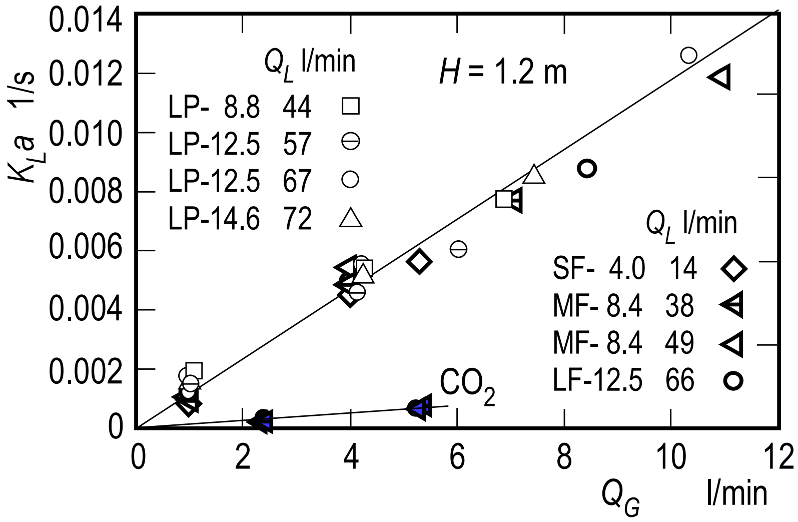
0.014
0.012
0.010
0.008
0.006
0.004
0.002
0
K_La 1/s
Q_L l/min
LP- 8.8 44
LP-12.5 57
LP-12.5 67
LP-14.6 72
H = 1.2 m
Q_L l/min
SF- 4.0 14
MF- 8.4 38
MF- 8.4 49
LF-12.5 66
CO_2
0
2
4
6
8
10
12
Q_G l/min

(a)

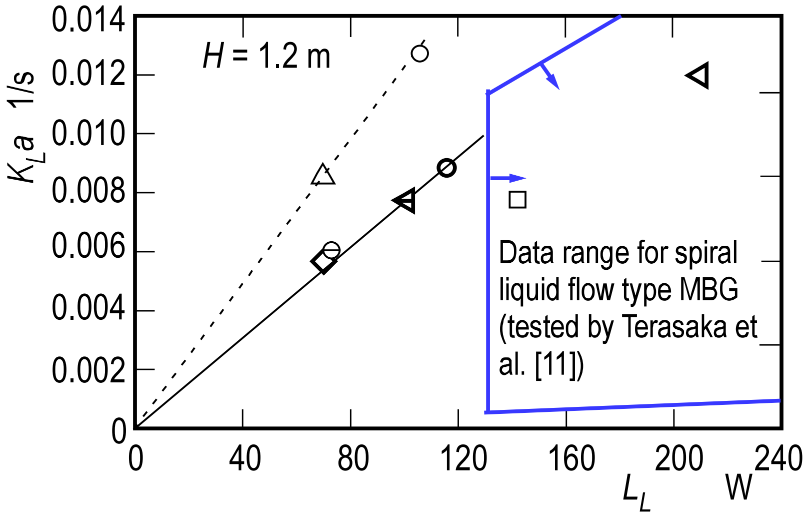
0.014
0.012
0.010
0.008
0.006
0.004
0.002
0
K_La 1/s
H = 1.2 m
Data range for spiral liquid flow type MBG (tested by Terasaka et al. [11])
0
40
80
120
160
200
240
L_L W

(b)

Fig. 8.

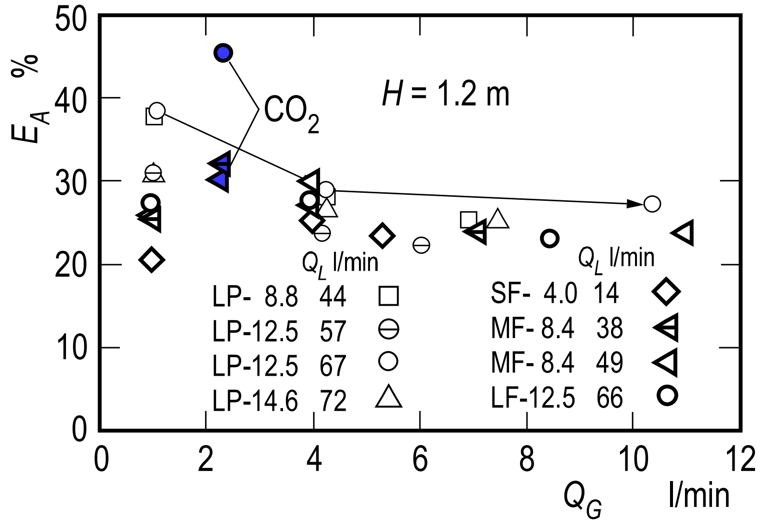

50
40
30
20
10
0
E_A %
0
2
4
6
8
10
12
Q_G l/min
H = 1.2 m
CO_2
Q_L l/min
LP- 8.8 44
LP-12.5 57
LP-12.5 67
LP-14.6 72
Q_L l/min
SF- 4.0 14
MF- 8.4 38
MF- 8.4 49
LF-12.5 66

Fig. 9.

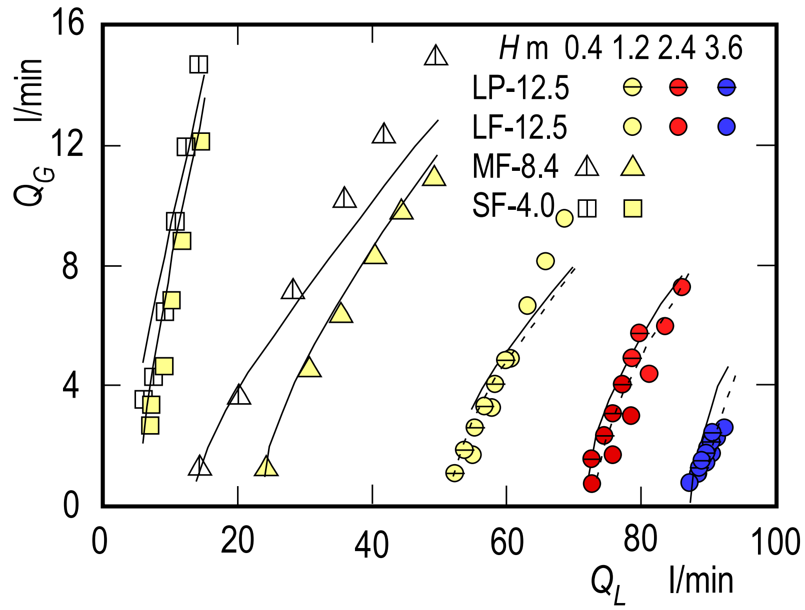

16
12
8
4
0
0
20
40
60
80
100
Q_G l/min
Q_L l/min
H m 0.4 1.2 2.4 3.6
LP-12.5
LF-12.5
MF-8.4
SF-4.0

(a)

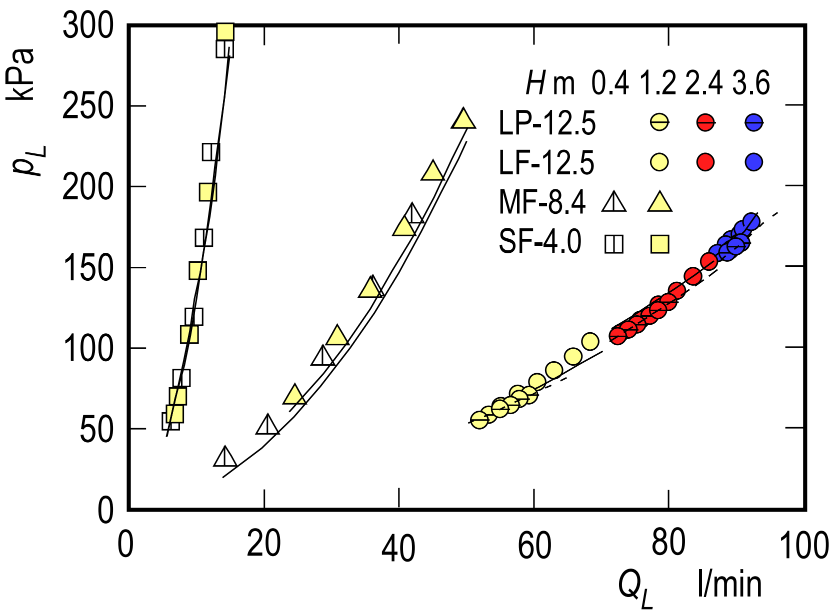

300
250
200
150
100
50
0
0
20
40
60
80
100
p_L kPa
Q_L l/min
H m 0.4 1.2 2.4 3.6
LP-12.5
LF-12.5
MF-8.4
SF-4.0

(b)

Fig. 10.

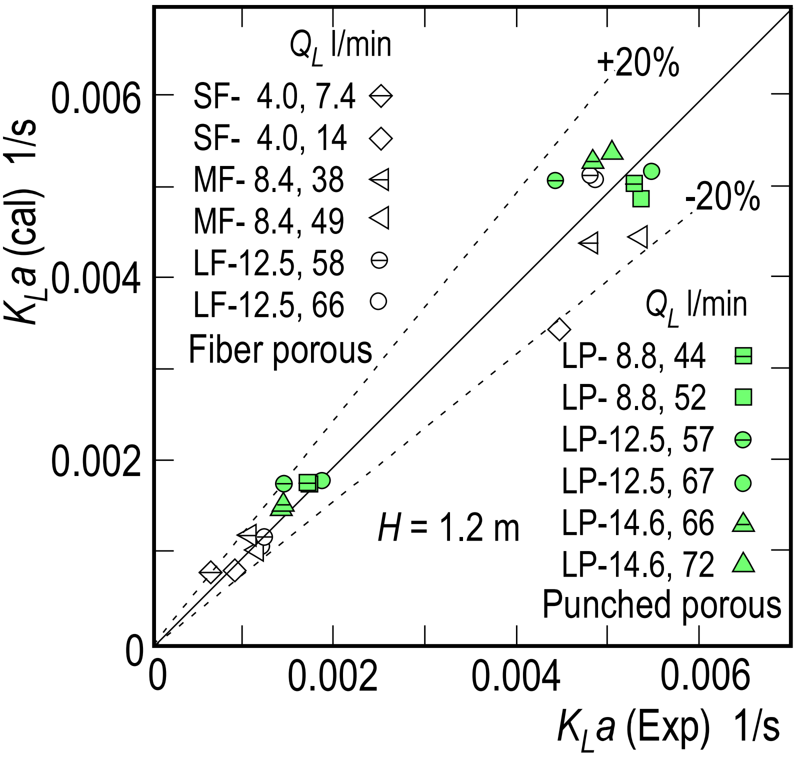

Q_L l/min
SF- 4.0, 7.4
SF- 4.0, 14
MF- 8.4, 38
MF- 8.4, 49
LF-12.5, 58
LF-12.5, 66
Fiber porous
+20%
-20%
Q_L l/min
LP- 8.8, 44
LP- 8.8, 52
LP-12.5, 57
LP-12.5, 67
LP-14.6, 66
LP-14.6, 72
Punched porous
H = 1.2 m
0.006
0.004
0.002
0
K_La (cal) 1/s
K_La (Exp) 1/s

Fig. 11.

List of Tables

Table 1

MBG type	Porous	D mm	d_o mm	β^2 -	l mm	d_G μm	h_G mm	A_H mm^2
LP-8.8	Punched	22	8.8	0.16	8	300	0.2	152.7
LP-12.5			12.5	0.323				
LP-14.6			14.6	0.44				
SF-4.0	Fiber	7	4.0	0.327	3-8	25	1.5	unknown
MF-8.4		14.7	8.4	0.327				
LF-12.5		22	12.5	0.323				

Table 2

Type	LP-8.8	LP-12.5	LP-14.6	LF-12.5	MF-8.4	SF-4.0
ζ_1	55.8	12.2	5.9	14.5	11.7	9.2
ζ_2	30.4	5.0	1.6	4.6	4.6	3.7
ζ_3	1700	1700	1700	4000	4000	4000

***Detailed Response to Reviewers**

Ms. Ref. No.: ETFS-D-11-00485

Title: Micro-bubble generation rate and bubble dissolution rate into water by a simple multi-fluid mixer with orifice and porous tube Experimental Thermal and Fluid Science

To Reviewer #1:

Thank very much for giving the authors a lot of good comments. According to the reviewer's comments, the authors revised the manuscript as written in red characters. In addition, the answers to the respective comments are as follows:

1. The number of reference does not coincide with its order of citation in the main body.

   We changed the citation number just above Eq. (3) to [10] and that just above Eq. (10) to [14].

2. Measurement uncertainties in flow rates, pressure, bubble diameter, concentration of oxygen/carbon dioxide and mass transfer coefficients much be clearly described in the manuscript.

   We added them in sections 2.2 to 2.5.

3. The authors described that averaged value of the two axes was taken as the bubble diameter" in page 4, line 20 -21. This is not correct as the volume-equivalent bubble diameter for ellipsoidal bubbles. How much is the maximum or minimum aspect ratio of a bubble? Why the authors assume spheroid shape to calculate bubble diameter?

   We added sentences in 2.4. Most bubbles were spherical as described in the original manuscript. Over about 1.5 mm, however, a little distorted bubbles appeared, but the aspect ratio was within 1.2. Why the authors assume spheroid bubble is that the interfacial area-equivalent bubble diameter is more important than the volume-equivalent bubble diameter for discussing bubble dissolution in water. In addition, the difference in bubble diameter between the interfacial area-equivalent and the volume-equivalent is negligibly quite small for the present bubbles.

4. Measurement method of concentration of carbon dioxide is not described. The method and its uncertainty must be described in the manuscript.

   We added them in section 2.5.

5. Although the authors described "LP-8.8 gives the largest QG t a fixed QL because the water pressure

in the air suction section becomes the lowest at a fixed QL" in page 5, line 48 - 49, LP-8.8 did not work at H = 2.4 and 3.6 m as mentioned in page 5, line 36. Why?

We added the reason in section 3.1. As you can see from Fig. 3 (b), the water pressure at the MGB inlet increased with the water depth, *H*, and the water flow rate, Q_L, thus in order to generate micro-bubbles at *H* = 2.4 and 3.6 m much larger water power must be supplied than that given by the present water circulation pump.

6. The authors described "LP-12.5 is superior to others at H > 2/4 in page 5, the last line. However, LP14.6 realizes higher QG at the constant LL than LP12.5 judging from Fig. 3 (c), and therefore, LP14.6 has better performance than LP12.5.

As to Fig. 3 (c) we modified the explanation and added one reference in section 3.1.

7. There is no explanation of experiment using double SF-4.0/MF-8.4. Did the two MBG locate in parallel or tandem?

We added a sentence in section 3.3. Two MBGs are assumed to be placed at the same water depth.

8. In the concentration measurement of oxygen, is there no influence of dissolution of ambient air through the water surface in the tank. How much is the time scale of the dissolution of oxygen through the water surface?

The effect of the oxygen dissolution from the free water surface is negligible, because the interfacial area in the free water surface is extremely smaller than that in the total of micro-bubbles.

9. The description "the increase of the concentration is low" is vague, because the magnitude of the gradient is large due to large difference between C and Cs. The authors mentioned that KLa for carbon dioxide case is unexpectedly small in page 7, line 23. It is recommended to add available literatures on KLa of CO2.

The reviewer misread “slow” as “low”, but we modified a little as “very slow”. There is no open data on K_La for CO_2 micro-bubbles, as we know. Why we wrote “unexpectedly small” is that we had had a prejudice CO_2 to be an easily dissolve into water as lemonade and cola.

10. Judging from Fig. 8 (b), LP12.5 with QL = 57 shows lower performance than LP14.6 and LP12.5

with QL = 67, although the authors mentioned that LP-12.5 and LP14.6 type with punched porous are superior to others in page 7. Line 37 - 38.

We added Q_L values there.

11. In Fig. 6 (a) and (b), there is large difference in the total number of bubbles for QG = 1.0 l/min between LP-12.5 and LF-12.5, whereas the difference in bubble size is very small. Why? Does the mass flow rate evaluated from measured bubble size and bubble number coincide with the gas flow rate?

The gas flow rate measured does not coincide with that determined from bubble diameter and bubble number data since the bubble diameter was measured only for bubbles taken by several pictures. In order to obtain reliable bubble diameter distribution in the present measurement, 350 bubbles are sufficient as added in section 2.4. Thus, the number of 817 and 864 in Fig. 6 (a) were too many and time consuming for the measurement.

12. Most of conclusions seem to be just results for the present experimental apparatus and conditions. Applicability of the knowledge to the other MBG or micro-bubble systems is unclear. It is strongly recommended to add discussions on physical background of the results.

We added sentences in chapter 5.

Reviewer #2: The paper describes on generation and dissolving rates of micro-bubbles formed by the authors' prepared bubbler. The paper includes an interesting information for readers of this journal and acceptable after minor revision as pointed out below;

Thank very much for giving the authors good comments. According to the reviewer’s comments, the authors revised the manuscript as written in red characters. In addition, the answers to the respective comments are as follows:

1) Description on the details of porous materials and measurements of micro-bubbles is insufficient. The authors should to describe more details on those matters.

For porous materials, we added their names in section 2.1. For micro-bubble measurements, we added sentences in 2.4.

2) English is necessary to be polished up by native speakers who can understand the scientific contents.

Several sentences are corrected according to the advice.